

Modeling Overhead Transmission Line with Large Asymmetrical Spans

Leonardo Souza, Antonio Lima, Sandoval Carneiro Jr.

Abstract— In this paper we analyze the behavior of asymmetrical spans such as the ones found in wide river crossing or in overhead lines with wide spans. In the frequency domain, a non-uniform line can be represented by a cascade connection of uniform lines with distinct heights. This leads to a computationally inefficient line model in time-domain. In the frequency domain, the chain matrix can be used to improve the efficiency as an equivalent for the whole span can be obtained. This equivalent is a multi-input multi-output frequency dependent network. An analysis of the impact of the non-uniform span in an otherwise uniform line is investigated. To obtain time-domain responses, the Numerical Laplace Transform is used. Several configurations are considered, including an unconventional line with a very high SIL (Surge Impedance Loading). The results indicate that depending on the “type” of span considered very distinct transients waveforms can appear. These waveforms have very little in common with the ones found when a uniform line is considered.

Keywords: transmission line modeling, non-uniform lines, frequency domain, asymmetrical spans

I. INTRODUCTION

IN developing countries such as those of the so-called BRIC (Brazil, Russia, India, China) there is the challenge to transmit bulk power over large distances. For instance, there are some possible river crossings for overhead lines that will be constructed to connect the power generation in the Amazon Basin to the main load centers in the Southeast or Northeast part of the country. These river crossings are in the order of 2 km leading to very tall towers and wide line spans. For the analysis of the voltage/current surge propagation near such crossings a more detailed line modeling might be needed. Typically in modeling overhead lines all the conductors are assumed to be at a constant height. This leads to the so-called uniform line model where the line can be represented either by the Method of Characteristics (MoC – also known as the travelling wave method) or a nodal admittance matrix (Y_{nod}). In the uniform line case using MoC any transmission line can be represented using the appropriate admittance matrix and a propagation matrix also known as voltage deformation matrix.

When Y_{nod} is used, an n conductor line can be modeled using two block matrices, one containing the diagonal block submatrices and other the off diagonal submatrices. While MoC has been the preferred approach for time-domain modeling [1], frequency domain methods use the Y_{nod} approach [2]. A nonuniform line (NUL) can be considered as a generalization of the uniform line when the heights of the conductors are no longer assumed constant. This is the case of line spans found in river crossings, valleys or straits. Until recently, a direct approach for representing a NUL either in time-domain or frequency-domain modeling, demanded a discretization of the line in a number of segments of uniform lines. The main drawback of this approach is that a heavy computational burden may occur in time-domain as the segmentation demands the time-step to be smaller than the fastest mode found in the uniform lines. If the frequency domain is used, a more compact realization can be obtained using the chain matrix [2]-[3]. The segmented uniform lines matrices are converted to a matrix transfer function also known as chain matrix (Q_i) with the A_i , B_i , C_i , D_i constants. The cascade connection of Q_i leads to a single matrix which then can be converted to a nodal admittance matrix. This approach has been used to represent underground cable systems with cross-bonding [4] as well as in analyse of incident field excitation in overhead lines [5].

A distinct approach has been proposed in [6] where the A , B , C , D constants in the quadrupole matrix are obtained from the integration of the frequency domain differential equation of transmission lines. Simple linear algebra expressions can then be used to convert the A , B , C , and D constants to Y_{nod} . A time-domain model using this methodology was presented in [7].

In this paper we investigate the propagation characteristics of two NUL. The first one is a conventional 230 kV line and the second one is an unconventional line with a high SIL. The Numerical Laplace transform [8] was used to obtain the time-domain response. The paper is organized as follows: Section II presents a brief overview of nonuniform line modeling adopted here; Section III presents the test cases results. Section IV presents the main conclusions of this work.

II. NONUNIFORM LINE MODELING

A NUL can be modeled in the frequency domain using the same voltage/current differential equation as uniform lines. The main difference is that for a uniform line the impedance and admittance matrices per unit length also vary along the line. Equation (1) shows the expressions defining the voltage and current vectors for a multi-phase line.

This work was supported in part by grants from CNPq, Conselho Nacional de Desenvolvimento Científico e Tecnológico, Brasil, and from FAPERJ, Fundação Carlos Chagas Filho de Amparo à Pesquisa do Estado do Rio de Janeiro, Rio de Janeiro, Brazil
L. A. Souza, A. Lima and S. Carneiro Jr. are with Universidade Federal do Rio de Janeiro, Rio de Janeiro, Cx. Postal 68504, CEP: 21945-970, Brazil (e-mail: acsl@dee.ufrj.br, leoas@hotmail.com, sandoval@dee.ufrj.br).

Paper submitted to the International Conference on Power Systems Transients (IPST2011) in Delft, the Netherlands June 14-17, 2011

$$\begin{aligned}\frac{d\mathbf{V}}{dx} &= -\mathbf{Z}(x)\mathbf{I} \\ \frac{d\mathbf{I}}{dx} &= -\mathbf{Y}(x)\mathbf{V}\end{aligned}\quad (1)$$

Differentiating (1) with respect to x leads to (2).

$$\begin{aligned}\frac{d^2\mathbf{V}}{dx^2} &= -\frac{d\mathbf{Z}(x)}{dx}\mathbf{I} - \mathbf{Z}(x)\frac{d\mathbf{I}}{dx} \\ \frac{d^2\mathbf{I}}{dx^2} &= -\frac{d\mathbf{Y}(x)}{dx}\mathbf{V} - \mathbf{Y}(x)\frac{d\mathbf{V}}{dx}\end{aligned}\quad (2)$$

Unlike the uniform line, there is no analytical solution. In the past finite differences have been used [9] and numerical integration can be used [6]. Another possibility is to assume that \mathbf{Z} and \mathbf{Y} have an exponential dependency with respect to x . This procedure is commonly known as exponential line as has been applied to lossless lines [10], lossy lines [11] and frequency-dependent tower models [12][13]. An alternative procedure is the segmentation of the nonuniform line in smaller, pseudo-uniform lines. If the line is segmented in such a way as the variation in both \mathbf{Z} and \mathbf{Y} can be disregarded, the chain matrix can be used [3][14].

Consider the nonuniform line represented schematically in Fig. 1. The NUL is segmented in several uniform lines with constant heights. The average height of the line segment is used in each chain matrix.

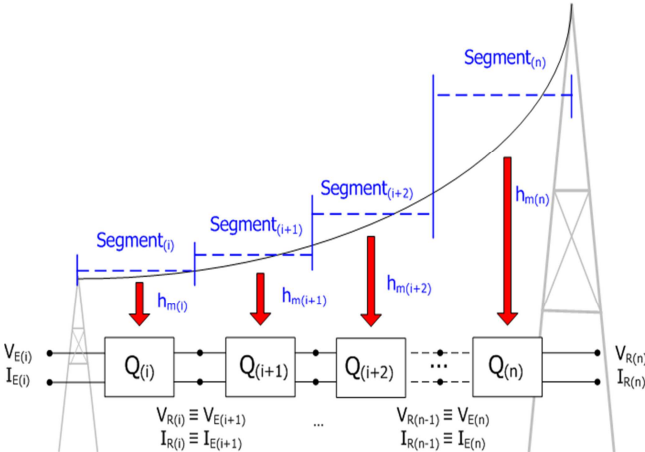


Fig. 1. Schematic representation of a nonuniform line with the chain matrix representation.

Traditionally the height of a conductor can be determined using the parabolic approximation of the catenary. However, it was found that in case of very wide spans, over 1 km, there were some noticeable differences [15]. Therefore, it was decided to use the catenary equation where the height of a conductor along the span is given by

$$y = q \left(\cosh\left(\frac{x}{q}\right) - 1 \right) \quad (3)$$

where q is the “specific weight” of the conductor. Thus phase-conductors will present distinct sags when compared with ground wires. The constant height h_m of the conductors to be used in each segment Q_i (see Fig 1) is obtained by the integration of (3), leading to

$$h_m = \frac{q^2 \left(\sinh\left(\frac{x_1}{q}\right) - \sinh\left(\frac{x_0}{q}\right) \right)}{x_1 - x_0} + q \quad (4)$$

where x_1 and x_0 are the x -coordinates that define the length of the uniform line approximation.

The procedure to obtain the equivalent nodal admittance matrix is rather straightforward. In order to define the number of segments the Courant-Friedrichs-Lewvy, CFL, criterion was adopted [14]. This criterion stipulates that the minimum length Δx for the uniform segment is given by

$$\Delta x \geq v \Delta t \quad (5)$$

where v is the speed of the fastest mode. In this work the speed of light was adopted. Another possible criterion for the determination of Δx is to compare the line parameters obtained with those using the cylindrical electrode formulation [16] or the finite-length parameter methodology [18][21]. This comparison is left for future research.

After the length of uniform segment is determined we obtain the nodal admittance matrix of each segment, i.e., the nodal admittance of a uniform line which is given by

$$\mathbf{Y}_{nod} = \begin{bmatrix} \mathbf{Y}_{11} & -\mathbf{Y}_{12} \\ -\mathbf{Y}_{21} & \mathbf{Y}_{22} \end{bmatrix} \quad (6)$$

with $\mathbf{Y}_{11} = \mathbf{Y}_{22}$ and $\mathbf{Y}_{12} = \mathbf{Y}_{21}$ and can be defined in the phase domain by

$$\mathbf{Y}_{11} = \mathbf{Y}_c (\mathbf{I} + \mathbf{H}^2) (\mathbf{I} - \mathbf{H}^2)^{-1} \quad (7)$$

$$\mathbf{Y}_{12} = 2\mathbf{Y}_c (\mathbf{I} - \mathbf{H}^2)^{-1}$$

where \mathbf{Y}_c is the characteristic admittance matrix and \mathbf{H} is the propagation function matrix also known as voltage deformation matrix. By using the matrix relation shown in (8) the chain matrix of each uniform line segment is obtained.

$$\mathbf{Q} = \begin{bmatrix} \mathbf{A} & \mathbf{B} \\ \mathbf{C} & \mathbf{D} \end{bmatrix} = \begin{bmatrix} \mathbf{Y}_{21}^{-1} \mathbf{Y}_{22} & \mathbf{Y}_{21}^{-1} \\ -\mathbf{Y}_{12} + \mathbf{Y}_{11} \mathbf{Y}_{12}^{-1} \mathbf{Y}_{22} & \mathbf{Y}_{11} \mathbf{Y}_{21}^{-1} \end{bmatrix} \quad (8)$$

By cascading each transfer matrix an equivalent input-output matrix transfer function of the nonuniform line is derived. This can then be converted to an equivalent nodal admittance matrix as shown in (9).

$$\mathbf{Y}_{nod_{eq}} = \begin{bmatrix} \mathbf{D}_{eq} \mathbf{B}_{eq}^{-1} & \mathbf{C}_{eq} - \mathbf{D}_{eq} \mathbf{B}_{eq}^{-1} \mathbf{A}_{eq} \\ -\mathbf{B}_{eq}^{-1} & \mathbf{B}_{eq}^{-1} \mathbf{A}_{eq} \end{bmatrix} \quad (9)$$

It can be proved that (9) is symmetrical [3], thus only three block matrices of $\mathbf{Y}_{nod_{eq}}$ need to be calculated.

To avoid numerical instabilities it is possible to obtain these results using only the smallest eigenvalues in (6). References [3] and [4] present more details in that matter.

III. TEST CASES

The first case considered is the same as in [6][7]. It is a horizontal line in which adjacent conductors are 10 m apart. The conductor radius is 2.54 cm. The water resistivity is 10 $\Omega \cdot m$. Fig. 2 depicts this configuration.

A step voltage of 1 V is applied at terminal #1 while terminal #2 remains open. The CFL criterion indicates that the uniform lines segments should be 30 m in length.

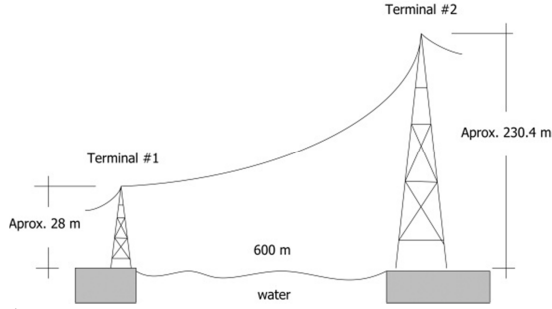


Fig. 2. First test case

Fig. 3 shows the output on the outside phase conductor at terminal #2. If this curve is compared with Fig. 11 in [7] it seems to be a considerable agreement.

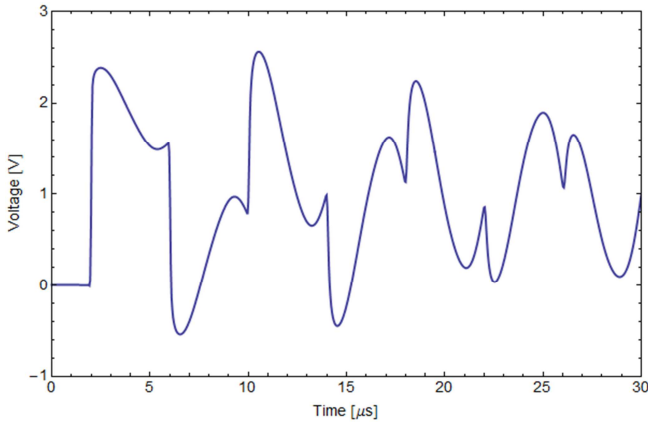


Fig. 3. Voltage at the first phase of terminal #2 for a step voltage at terminal #1

This case was also used to assess the voltage mismatches as a function of the number of chain matrices used to obtain the NUL equivalent. The case using 30 chain matrices is used as a base of comparison. Table I summarizes this comparison where N is the number of chain matrices, ℓ is the length of the uniform line segment and $\text{Max}(\Delta V)$ stands for the maximum voltage mismatch found in the simulation.

TABLE I – MISMATCH IN VOLTAGES AS FUNCTION OF THE NUMBER OF CHAIN MATRICES USED

N	ℓ	$\text{Max}(\Delta V)$
20	30	0.0238651
30	20	0
40	15	0.00679813

It is interesting to note that a NUL is not “symmetrical” in terms of input/output relationships. For instance, if the step voltage is applied at terminal #2 the output is different from the one we obtained applying the step at terminal #1. To illustrate this behavior, consider a case where the same three-phase step voltage is applied at terminal #2. The result is depicted in Fig. 4 where it is seen that although the voltage maxima are similar, the waveforms are considerably different.

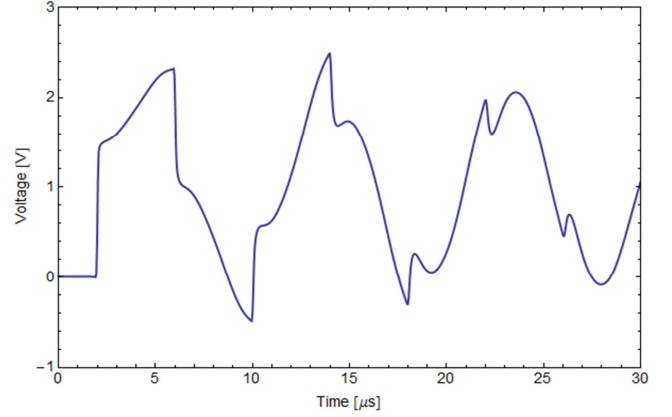


Fig. 4. Voltage at the first phase of the term. #1 for a step voltage at term. #2

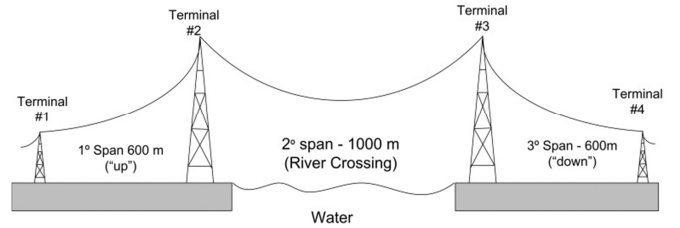


Fig. 5. Schematic of a full river crossing – second test case

The second case considered is a so-called “full river crossing,” consisting of three NULs as depicted in Fig. 5, two over ground and one over water. For this case the ground resistivity considered was $1000 \Omega \cdot \text{m}$ and the water resistivity was the same as in the previous case. Again a three-phase step voltage 1 V was applied to terminal #1 while terminal #4 remained open, as shown in Fig. 5. Two strategies were considered for the analysis of this configuration:

- Modeling each span in Fig. 5 by a NUL;
- Modeling the “up” and “down” spans using NUL while the second span, the actual river crossing, is modeled using a uniform line.

The second span in this case is symmetrical with respect to the mid-span so we decided to investigate if we could approximate the NUL by a uniform line (UL). The results are depicted in Fig. 6. Case (a) is shown as a solid line while case (b) is presented as a dashed line.. As expected case (a) showed higher oscillations and although the maxima are close, mainly after 20 ms, the waveforms are rather distinct. The UL approximation of the second span lead to a results with a distinct waveform, although the highest values found in both cases were very close.

Even though not yet considered in these two cases, the presence of ground wires can significantly affect the voltage waveforms. Fig. 7 shows the voltage at terminal#2 for the first case when the overhead line has ground wires. These were 3/8” EHS, located 5 meters above the phase conductors and seven meters away for the central phase. These coordinates were obtained by applying the electrogeometric model. The ground-wires were assumed grounded at the tower for this analysis. As it can be seen the waveform is now much “smoother” and with considerably lowers peaks.

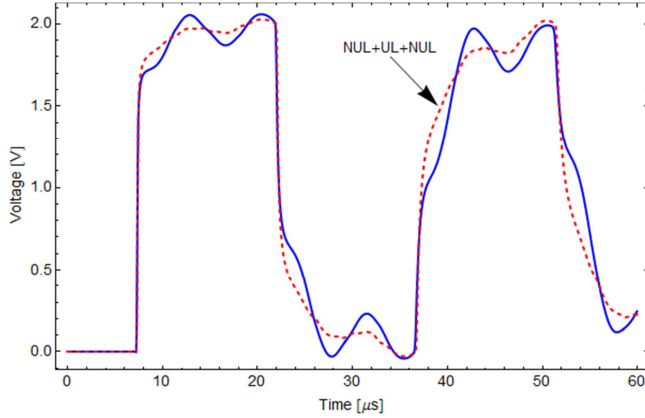


Fig. 6. Voltage output for a full river crossing

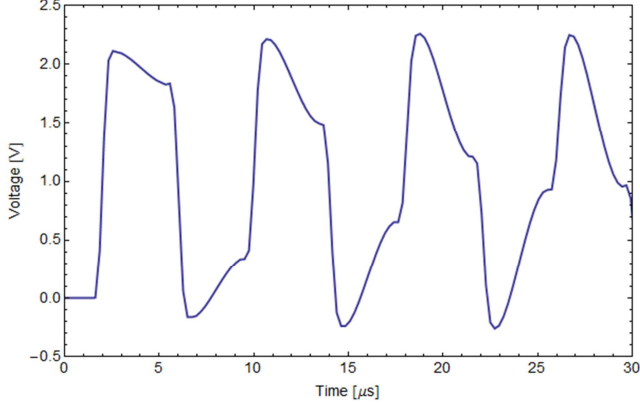


Fig. 7. Voltage at the first phase of terminal #2 for a step voltage at terminal #1 considering ground wires

The last case considered is shown in Fig. 9, which is typical of a large river crossing as can be found in the Amazon Basin. In this case, the distance from shore to shore may be higher than 2 km, it should be point out that the Amazon river and some of its affluent are much wider at other location. The line configuration is shown in Fig. 8 with the conductors at the minimum height. It is essentially the same circuit that was used in [19] but with a higher nominal voltage. It is a 1000 kV overhead line with a nominal power of 8 GW. Phase conductors are Bluejay and ground wires are 3/8" EHS. The line has an unusual bundle arrangement to maximize the transmitted power. More details regarding the line design can be found in [20].

Fig. 9 depicts a possible configuration for the crossing of a wide river. In the first scenario we consider for both the first and third spans a constant resistivity ground as in the other cases, 1000 $\Omega \cdot m$. A second scenario was the application of a more detailed soil model for these spans. In this case, the frequency dependency on both ground conductivity and permittivity is considered [21]. This type of soil modeling is based on experimental measurements firstly carried out in the Amazon region, thus being more than suitable for the analysis of a possible transmission system in this area. In Appendix A some basic information on the frequency dependent soil model is provided.

For the second span, over water, a simple, pure conductivity soil model was used with the same parameter as before. The ground wires were assumed continuously

grounded, i.e. grounded at every tower. As before, a three-phase step voltage is applied to terminal #1 while terminal #4 remains open.

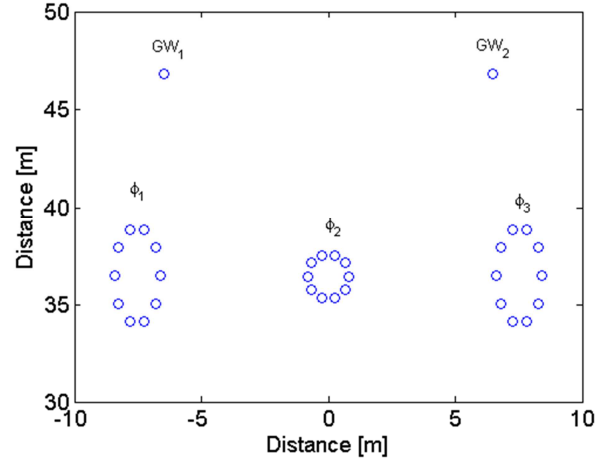


Fig. 8. Voltage at the first phase of terminal #2 for a step voltage at terminal #1 considering ground wires

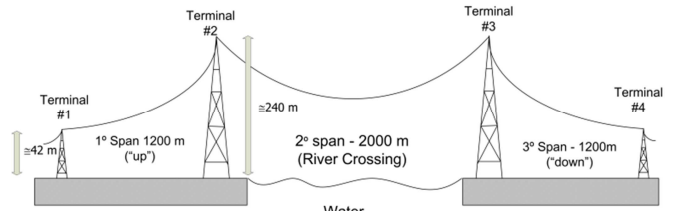


Fig. 9. Schematic for a wide river crossing

Fig. 10 shows the voltage output in the outside phase on terminal #4. It can be seen that the presence of ground wires and a more detailed soil modeling has decreased the highest peaks and created a highly damped voltage. The effect of the soil in NUL seems to affect mainly the amplitude.

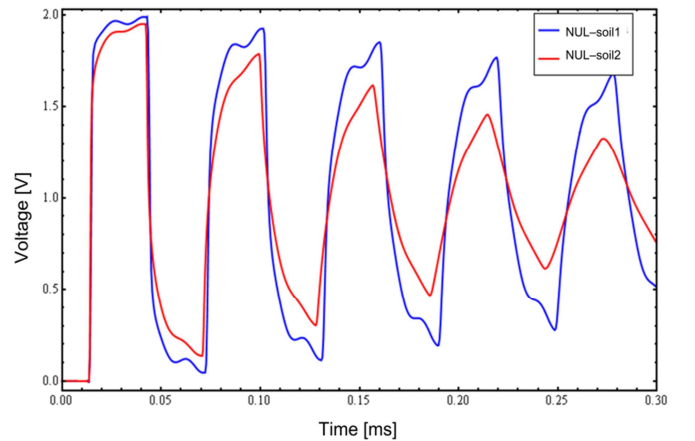


Fig. 10. Voltage at terminal #4, first phase, considered two soil modeling for the first and third spans.

IV. CONCLUSIONS

This work has focused on the analysis of the voltage propagation characteristic of NUL. The NUL was obtained by a cascade of several uniform line segments with distinct

heights. An analysis of a simple case each with a distinct number of chain matrices indicated that a rather simple approach can be used to determine the minimum length of the uniform line to be used.

The presence of NUL increases the voltage oscillations and introduces distinct frequency oscillations. If the NUL presents some symmetry its impact is considerably lower, i.e., the presence of symmetrical spans tends to minimize the effect of the NUL.

The overall behavior of the overhead lines was essentially the same, regardless of conductor (bundle) arrangement. The line with a high SIL and non-identical bundles presents waveforms quite similar to those found for the case of a single conductor overhead line.

The presence of ground wires has a pronounced effect of the voltage attenuation thus being a key element for the overvoltage analysis of a NUL system involving an asymmetrical span.

Future research considering the response of the lines having high SILs at high frequencies is still needed. For instance, the influence of the tower and of the tower grounding on the behavior to the voltage remains to be determined.

V. APPENDIX A

The ground propagation constant is given by

$$\gamma_s = \sqrt{j\omega\mu(\sigma + j\omega\epsilon)} \approx \sqrt{j\omega\mu\sigma}$$

as for a purely resistive soil is assumed $\sigma \gg \omega\epsilon$. For the case where the frequency dependent soil is considered the model is represented by an imittance $\kappa(\omega)$ given by

$$\kappa(\omega) = \sigma + j\omega\epsilon = \sigma_0 + \delta_\sigma + j\delta_{\omega\epsilon}$$

where σ_0 is the low frequency soil conductivity in S/m and can be obtained by conventional techniques. Despite its simplicity this model has provided accurate representation of different sites, with distinct soil and geological structures. The part responsible by the frequency dependency in the soil parameters is given by

$$\delta_\sigma + j\delta_{\omega\epsilon} = \Delta \left(\frac{f}{10^6} \right)^\alpha \left(\cot \left(\alpha \frac{\pi}{2} \right) + j \right)$$

In the expression above both Δ and α are constant. These parameters were determined assuming a Weibull distribution of the soil samples. For the cases considered here we have used a specific set of measurement which led to

$$\Delta = 8.92028 \cdot 10^3 \quad \alpha = 0.71603$$

Thus the ground imittance to be used in the evaluation of the line parameters is given by

$$\kappa(\omega) = 10^{-3} + \omega^{0.71603} (0.057849 + j0.12097) 10^{-6}$$

with the value of $\kappa(\omega)$ the ground propagation constant is obtained for every frequency. The line parameters can be obtained using the Gaussian quadrature of the infinite integrals in Carson's formulation. If the complex ground plane is to be used, complex penetration depth is defined by the following.

$$p = \sqrt{(j\omega\mu\kappa(\omega))^{-1}}$$

VI. REFERENCES

- [1] B. Gustavsen, G. Irwin, R. Mangelrod, D. Brandt and K. Kent, "Transmission line models for the simulation of interaction phenomena between parallel AC and DC overhead lines," *In Proc. of IPST'99 International Power System Transients Conference*, Budapest, Hungary, 1999, available at <http://www.ipst.org>
- [2] L. Wedepohl, The theory of Natural Modes in Multiconductor Transmission Systems, Tech. rep., the University of British Columbia, 1997.
- [3] L. M. Wedepohl and C. S. Indulkar, Wave propagation in nonhomogeneous systems – Properties of the chain matrix, *Proc. of IEE*, vol. 121, no. 9, Sept. 1974
- [4] L.M. Wedepohl, C. S. Indulkar, "Switching overvoltages in long crossbonded cable systems using the Fourier Transform", *IEEE Trans. on PAS*, v. PAS-98, pp. 1476–1480, 1979.
- [5] P. Gomez, P. Moreno, J. Naredo, "Frequency-domain transient analysis of nonuniform lines with incident field excitation," *IEEE Trans. on Power Delivery*, v. 20, n. 3, pp. 2273–2280, Jul. 2007.
- [6] A. Semlyen, "Some Frequency Domain Aspects of Wave Propagation on Nonuniform Lines", *IEEE Trans. on Power Delivery*, v. 18, n. 1, pp. 315 - 322, January 2003.
- [7] A. Ramirez, A. Semlyen and R. Iravani, "Modeling nonuniform transmission lines for time domain simulation of electromagnetic transients", *IEEE Trans. on Power Delivery*, v. 18, n. 3, pp. 968–974, Jul. 2003.
- [8] D. J. Wilcox, "Numerical Laplace Transformation and Inversion", *International Journal Elect. Eng.*, v. 15, pp. 247–265, 1978.
- [9] S. Schelkunoff, "Electromagnetic waves," D. Van Nostrand Co., New York, 1943.
- [10] E. Oufi, A. AlFuhaid, M. Saied, "Transient analysis of lossless single-phase nonuniform transmission lines," *IEEE Trans. on Power Delivery*, v. 9, pp. 1694–1700, Jul. 1994.
- [11] A. AlFuhaid, E. Oufi, M. Saied, "Application of nonuniform-line theory to the simulation of electromagnetic transients in power systems," *Electric Power and Energy Syst.*, v. 20, n. 3, pp. 225–233, 1998.
- [12] H. Nguyen, H. Dommel and J. Marti, "Modeling of single-phase nonuniform transmission lines in electromagnetic transient simulations," *IEEE Trans. on Power Delivery*, vol. 12, pp. 916–921, Apr. 1997
- [13] J. Gutierrez, P. Moreno, J. Naredo, J. Bermudez, M. Paolone, C. Nucci, F. Rachidi, "Nonuniform transmission tower model for lightning transiente studies," *IEEE Trans. on Power Delivery*, v. 19, n. 2, Apr. 2004.
- [14] P. Gomez, P. Moreno, J. Naredo, "Frequency domain transiente analysis of nonuniform lines with incident field excitation," *IEEE Trans. on Power Delivery*, v. 20, n. 3, pp. 2273–2280, Jul. 2005.
- [15] L.A. Souza, "Study of nonuniform transmission lines in the frequency domain", Master's thesis, Dept. Electrical Engineering, Federal University of Rio de Janeiro, COPPE/UF RJ, 2009 [In Portuguese].
- [16] J. C. Salari Filho, C. Portela, "A Methodology for Electromagnetic Transients Calculation—An Application for the Calculation of Lightning Propagation in Transmission Lines," *IEEE Trans. on Power Delivery*, vol. 22, no.1, PP. 527–536, Jan. 2007.
- [17] A. Ametani, A. Ishihara, "Investigation of impedance and line parameters of a finite-length multiconductor system," *Trans. IEE Japan*, vol. 113-b, no.8, 1993
- [18] A. Ametani, "Wave propagation on a nonuniform line and its impedance and admittance," *The Science and Engineering Review of Doshisha University*, vol. 43, no.2, pp. 11–23, 2002
- [19] R. Dias, A. Lima, C. Portela, M. Aredes, "Non conventional transmission line with FACTS in electromagnetic transient programs," *In Proc. of IPST'2009 International Power System Transients Conference*, Kyoto, Japan, 2009, available at <http://www.ipst.org>
- [20] R. Dias, A. Lima, C. Portela, M. Aredes, "Extra Long Distance for Bulk Power Transmission," *IEEE Trans. on Power Delivery*, accepted for publication.
- [21] A. Lima, C. Portela, "Inclusion of Frequency-Dependent Soil Parameters in Transmission-Line Modeling", *IEEE Trans. on Power Delivery*, v. 22, n. 1, pp. 492–499, Jan. 2007.